Published in final edited form as:
Cell. 2013 February 28; 152(5): 1051–1064. doi:10.1016/j.cell.2013.01.051.

Regulation of WASH-Dependent Actin Polymerization and Protein Trafficking by Ubiquitination

Yi-Heng Hao[1,7], **Jennifer M. Doyle**[1,7], **Saumya Ramanathan**[1], **Timothy S. Gomez**[2], **Da Jia**[4], **Ming Xu**[3], **Zhijian J. Chen**[3,5], **Daniel D. Billadeau**[2], **Michael K. Rosen**[4,5], and **Patrick Ryan Potts**[1,6,*]

[1]Department of Physiology, UT Southwestern Dallas, TX 75390

[2]Department of Immunology and Division of Oncology Research, Mayo Clinic, Rochester, MN 55905

[3]Department of Molecular Biology, UT Southwestern Dallas, TX 75390

[4]Department of Biophysics, UT Southwestern Dallas, TX 75390

[5]Howard Hughes Medical Institute, UT Southwestern Dallas, TX 75390

[6]Department of Pharmacology, UT Southwestern Dallas, TX 75390

SUMMARY

Endosomal protein trafficking is an essential cellular process that is deregulated in several diseases and targeted by pathogens. Here, we describe a novel role for ubiquitination in this process. We find that the novel E3 RING ubiquitin ligase, MAGE-L2-TRIM27, localizes to endosomes through interactions with the Retromer complex. Knockdown of MAGE-L2-TRIM27 or the Ube2O E2 ubiquitin-conjugating enzyme significantly impaired Retromer-mediated transport. We further demonstrate that MAGE-L2-TRIM27 ubiquitin ligase activity is required for nucleation of endosomal F-actin by the WASH regulatory complex, a known regulator of Retromer-mediated transport. Mechanistic studies showed that MAGE-L2-TRIM27 facilitates K63-linked ubiquitination of WASH K220. Significantly, disruption of WASH ubiquitination impaired endosomal F-actin nucleation and Retromer-dependent transport. These findings provide a cellular and molecular function for MAGE-L2-TRIM27 and reveal novel aspects of retrograde transport, including an unappreciated role of K63-linked ubiquitination and identification of an activating signal of the WASH regulatory complex.

INTRODUCTION

Endosomal protein recycling pathways facilitate the transfer of membrane proteins from early and late endosomes back to the trans-Golgi network (TGN) or plasma membrane (Bonifacino and Rojas, 2006). In doing so, these pathways generally function to prevent lysosomal delivery and degradation of membrane proteins. Endosome-to-Golgi transport, referred to as retrograde transport, is an important cellular process that facilitates the

*Correspondence: Patrick Ryan Potts, 5323 Harry Hines Blvd, Dallas, TX 75390-9040, Ryan.Potts@UTSouthwestern.edu (214) 648-1493.

[7]These authors contributed equally

recycling of a variety of proteins, including: sorting receptors (such as CI-M6PR), SNARE membrane fusion proteins, membrane receptors, metabolite transporters, and several proteins that undergo polarized localization/secretion (Bonifacino and Rojas, 2006; Johannes and Popoff, 2008). Importantly, retrograde transport has been implicated in a number of different human pathologies. Endosome-to-Golgi transport is essential for cellular entry of pathogenic toxins, such as Shiga, Cholera, and ricin, as well as viral pathogens such as HIV (Brass et al., 2008; Sandvig and van Deurs, 2005). Furthermore, components of the retrograde transport pathway are downregulated in Alzheimer's disease and upregulated in cancer (Scott et al., 2009; Small, 2008).

Recent studies have started to define the molecular machinery crucial for different aspects of this process, including cargo recognition, endosomal membrane budding, tubulation, and scission, and vesicle transport, tethering, and fusion at the TGN (Bonifacino and Rojas, 2006; Cullen and Korswagen, 2012). One critical component is the Retromer protein complex that consists of VPS26, VPS29, and VPS35 and functions to recognize retrograde cargo on endosomes (Bonifacino and Hurley, 2008). Another essential factor in retrograde transport is WASH. WASH is a member of the Wiskott-Aldrich syndrome protein (WASP) family consisting of WASP/N-WASP, WAVE, WHAMM, JMY, and WASH (Campellone and Welch, 2010). Like other WASP family members, WASH contains a carboxy-terminal VCA (verprolin homologous or WH2, central hydrophobic, and acidic) motif that binds to actin and the Arp2/3 complex to stimulate actin filament nucleation (Derivery et al., 2009; Duleh and Welch, 2010; Jia et al., 2010; Linardopoulou et al., 2007; Liu et al., 2009). Recent studies have demonstrated that WASH is endosomal-associated, exists in a macromolecular complex termed the WASH Regulatory Complex (SHRC) and functions downstream of the Retromer complex to facilitate endosome-to-Golgi transport (Derivery et al., 2009; Duleh and Welch, 2010; Gomez and Billadeau, 2009; Linardopoulou et al., 2007). Importantly, Retromer and SHRC have been implicated in other endosomal recycling pathways, including endosome-to-plasma membrane sorting of integrins (Zech et al., 2011). SHRC consists of at least five core factors, CCDC53, FAM21, SWIP, Strumpellin, and WASH (Derivery et al., 2009; Gomez and Billadeau, 2009; Jia et al., 2010). The SHRC is recruited to early endosomes by multivalent interactions between repeat elements in FAM21 and the Retromer subunit VPS35 (Harbour et al., 2012; Jia et al., 2012). WASH is essential for Arp2/3-induced F-actin accumulation on endosomes (Derivery et al., 2009; Gomez et al., 2012). With WASH suppression, scission of membrane tubules emanating from endosomes was suggested to be impaired (Derivery et al., 2009; Gomez and Billadeau, 2009) and knockout of WASH in MEFs resulted in the collapse of the early endosomal and lysosomal networks (Gomez et al., 2012).

Nucleation of F-actin by WASP family members is regulated by a variety of signaling events that converge on VCA motif activation/exposure (Padrick and Rosen, 2010). The VCA motifs of WASP/N-WASP, WAVE and WASH are autoinhibited through intramolecular and intermolecular interactions (Chen et al., 2010; Ismail et al., 2009; Jia et al., 2010; Kim et al., 2000; Miki et al., 1998). Several signaling molecules have been identified to promote the activation/exposure of WASP/N-WASP and WAVE VCA motifs to allow timed and localized F-actin nucleation, including small GTPases Cdc42 and Rac1, PIP_2 and PIP_3 phospholipids, and phosphorylation by the Src, Abl, and Cdk family of kinases (Eden et al., 2002; Ismail et al., 2009; Kim et al., 2000; Lebensohn and Kirschner, 2009; Miki et al., 1998; Padrick and Rosen, 2010). Contrary to WASP/N-WASP and WAVE, the mechanisms regulating WASH activation have been more elusive. The Rho GTPase has been genetically linked to activation of WASH in Drosophila (Liu et al., 2009), but is not sufficient to directly activate human WASH in vitro (Jia et al., 2010). Ubiquitination is a post-translational modification in which a small 76 amino acid protein is

covalently attached to lysine residues in substrate proteins through a three step E1, E2, and E3 enzymatic cascade (Fang and Weissman, 2004).

Ubiquitination can have pleiotropic effects on its substrates depending on the length and type of ubiquitin chains. K48-linked ubiquitin chains typically target proteins for degradation by the 26S proteasome (Bochtler et al., 1999). However, K63-linked ubiquitination typically acts as a signaling event to modify function, such as altering protein-protein interactions or protein conformations, or targeting proteins for lysosomal delivery (Sun and Chen, 2004). Recently, we identified a novel class of proteins that bind to and enhance the activity of E3 RING ubiquitin ligases (Doyle et al., 2010). These ubiquitin ligase enhancers are known as melanoma antigen (MAGE) genes and comprise a family of over 50 unique human genes (Chomez et al., 2001). Although the biochemical function of MAGE proteins in ubiquitination has been elucidated, the cellular processes in which specific MAGE proteins act are unclear. Here we investigate the cellular function of MAGE-L2, a paternally imprinted gene that is abundantly expressed in the brain, maps to the Prader-Willi syndrome deletion locus, and is implicated in normal circadian rhythm and the hypothalamic-endocrine axis (Bischof et al., 2007; Boccaccio et al., 1999; Kozlov et al., 2007; Tennese and Wevrick, 2011).

RESULTS

Identification of MAGE-L2 E3 RING Ubiquitin Ligase Partner and Subcellular Localization

To determine the specific E3 RING ubiquitin ligase partner of MAGE-L2 and gain insight into its cellular function, we examined MAGE-L2 binding partners by tandem affinity purification (TAP) coupled to mass spectrometry. The E3 RING ubiquitin ligase TRIM27 was identified as a major binding partner of MAGE-L2 (Figure 1A). Binding of MAGE-L2 and TRIM27 was confirmed by reciprocal co-immunoprecipitation experiments (Figures 1B and S1C). Moreover, in vitro translated MAGE-L2 bound recombinant GST-TRIM27 but not GST alone, indicating the interaction between the two proteins is direct (Figure 1C). To confirm the association of MAGE-L2 and TRIM27, we stably expressed GFP-MAGE-L2 and mCherry-TRIM27 in U2OS cells and examined their co-localization by live cell microscopy. We found that the two proteins co-localized in discrete cytoplasmic puncta (Figure 1D), as well as in a smaller nuclear pool (data not shown). These findings suggest that TRIM27 binds MAGE-L2 and that the MAGE-L2-TRIM27 ubiquitin ligase complex localizes to discrete cytoplasmic structures.

MAGE-L2-TRIM27 Binds and Localizes to Retromer-Containing Endosomes

To determine the identity of the MAGE-L2-TRIM27 structures, we reanalyzed our mass spectrometry data of MAGE-L2 interacting proteins for clues. Interestingly, MAGE-L2 was identified to interact with VPS35 and VPS26 (Figure 1A), two components of the endosomal Retromer complex. mCherry-TRIM27 co-localized with GFP-tagged VPS35, VPS29, and VPS26, as well as the Retromer-associated SHRC proteins, WASH and FAM21 (Figure S1A). Furthermore, co-staining for endogenous VPS35 and TRIM27 clearly identified TRIM27 cytoplasmic structures as Retromer-positive endosomes (Figure 1E). Unfortunately, we were unable to observe endogenous MAGE-L2 due to the lack of specific, high quality antibodies (data not shown). More detailed analysis of TRIM27 localization revealed its localization to numerous tubular structures emanating from endosomes (Figure 1F), a property shared with the Retromer complex (Arighi et al., 2004; Bonifacino and Hurley, 2008). These findings suggest that MAGE-L2-TRIM27 localizes to the Retromer-positive subset of endosomes.

Next we confirmed the interaction between MAGE-L2-TRIM27 and the Retromer complex initially observed by mass spectrometry. MAGE-L2 and TRIM27 co-immunoprecipitated with all three components of the Retromer complex (Figures S1B–C and data not shown) and MAGE-L2 directly bound recombinant GST-VPS35 in vitro through its WH-B motif (Figures S1D and S1G–H). In addition, MAGE-L2 interaction with VPS35 did not impair VPS35 binding to the SHRC component FAM21 (Figure S1I). Furthermore, MAGE-L2-VPS35 interaction is functionally important, as knockdown of VPS35 dramatically inhibited MAGE-L2 and TRIM27 endosomal localization (Figures S1E–F and data not shown). These findings suggest that VPS35 recruits MAGE-L2-TRIM27 to Retromer-positive endosomes by binding to MAGE-L2.

MAGE-L2-TRIM27 Is Required for Endosomal Protein Recycling

We next assessed whether MAGE-L2-TRIM27 participates in endosome-to-Golgi transport. Two independent siRNAs targeting MAGE-L2 or TRIM27 were identified that significantly reduced their target protein's levels, but had no effects on the levels of other known essential factors required for retrograde transport (Figure S2A–C). Multiple siRNAs targeting MAGE-L2 or TRIM27 resulted in impaired CI-M6PR and TGN46 trafficking to a degree similar to VPS35-RNAi (Figures 2A–C and S2D). Importantly, the overall organization of the TGN was unaffected in MAGE-L2- or TRIM27-RNAi cells (Figure S2E). The steady state defects in CI-M6PR localization were corroborated by examining transport of a small pool of surface localized CI-M6PR to the TGN in MAGE-L2- and TRIM27-RNAi cells. MAGE-L2- or TRIM27-RNAi impaired transport of surface-labeled CI-M6PR to the TGN (Figure 2D). Importantly, the dispersed steady state or surface labeled CI-M6PR in TRIM27- or MAGE-L2-RNAi cells co-localized with the endosomal marker EEA1 (Figures 2E and S2F). Furthermore, CI-M6PR protein levels were reduced in MAGE-L2- and TRIM27-RNAi cells and Cathepsin D processing and trafficking were impaired (Figure 2F). Finally, overexpression of MAGE-L2 in combination with TRIM27 increased CI-M6PR endosomal retrieval kinetics (Figure S2G). These results suggest that MAGE-L2-TRIM27 is required for endosome-to-Golgi retrograde transport.

To extend our findings, we examined the requirement of TRIM27 on the trafficking of two additional physiologically and pathologically relevant substrates of the Retromer and SHRC complexes. First, knockdown of TRIM27 significantly impaired trafficking of the Retromer cargo cholera toxin subunit B (CTxB) to the TGN (Figure 2G). However, the trafficking of the SHRC-independent cargo Transferrin receptor to perinuclear recycling endosomes was unaltered in TRIM27-RNAi cells (Figure 2G) (Duleh and Welch, 2010; Gomez and Billadeau, 2009; Gomez et al., 2012). In addition, the Retromer and SHRC complexes have been implicated in the recycling of endosomal proteins to the plasma membrane, including integrins (Duleh and Welch, 2012; Zech et al., 2011). Therefore, we examined whether MAGE-L2 and TRIM27 function extends beyond endosome-to-Golgi trafficking by examining their contribution to the recycling of integrin α5 to the plasma membrane. Knockdown of MAGE-L2 or TRIM27 significantly decreased cell surface integrin α5 (Figure 2H) and increased the intracellular pool of integrin α5 in EEA1-negative endosomes (Figure 2I). Importantly, this decrease in cell surface integrin α5 in MAGE-L2- or TRIM27-RNAi cells is functionally significant, as invasion of cells through matrigel, a process regulated by integrins, is significantly impaired in MAGE-L2- or TRIM27-RNAi cells (Figure 2J). These results suggest that MAGE-L2-TRIM27 functions with the Retromer and SHRC complexes in both endosome-to-Golgi and endosome-to-plasma membrane protein recycling.

Ube2O E2 Ubiquitin-Conjugating Enzyme Is Required for Retrograde Transport

Next we determined whether the requirement for MAGE-L2-TRIM27 in retrograde transport involved its ubiquitin ligase activity by utilizing a TRIM27 RING mutant lacking E3 ubiquitin ligase activity. Unlike wild-type TRIM27, expression of an RNAi resistant TRIM27 RING mutant was unable to rescue retrograde transport of CI-M6PR in TRIM27-RNAi cells (Figures 3A and S3A). Importantly, the TRIM27 RING mutant localized similarly to the wild-type protein (Figure S3B). These results suggest that the ubiquitin ligase activity of MAGE-L2-TRIM27 is important for proper retrograde transport.

Next we examined which of the more than 35 different E2 ubiquitin-conjugating enzymes functions with MAGE-L2-TRIM27 to facilitate retrograde endosome-to-Golgi trafficking of CI-M6PR. Of the 35 E2 enzymes examined, knockdown of only Ube2O and Ube2L6 resulted in dramatic alteration of CI-M6PR localization (Figures 3B, S3C, and data not shown). Ube2O-RNAi showed similar penetrance as TRIM27-RNAi (Figures 3B–C), resulted in CI-M6PR dispersion to EEA1-positive endosomes (Figure 3D), and reduced total CI-M6PR (Figure 3E). However, Ube2L6-RNAi did not redistribute CI-M6PR to EEA-positive endosomes (Figure 3D) or promote lysosomal degradation of CI-M6PR (Figure 3E), but rather disrupted TGN organization (Figure S3D). Notably, Ube2O, but not Ube2L6, was also identified in a yeast-2-hybrid screen for E2 enzymes interacting with TRIM27 (Markson et al., 2009). These results suggest that the Ube2O E2 ubiquitin-conjugating enzyme is the physiologically relevant E2 enzyme functioning with MAGE-L2-TRIM27 in supporting retrograde transport.

Retrograde Transport Requires K63-Linked Ubiquitin Chains

We next investigated whether retrograde transport was dependent on ubiquitin, and if so, which type of poly-ubiquitin chain. To do so, we utilized the previously developed system (Xu et al., 2009) to inducibly knockdown ubiquitin by addition of tetracycline and replace it with a ubiquitin variant that is unable to produce a specific ubiquitin chain, namely ubiquitin in which lysine 48 or lysine 63 has been mutated to arginine (K48R or K63R, respectively; Figure S3E–F). We found that depletion of ubiquitin from cells dramatically affected CI-M6PR trafficking (Figures 3F and S3G). Addition of wild-type or K48R ubiquitin completely rescued CI-M6PR localization (Figures 3F and S3G), suggesting that ubiquitin is required for retrograde trafficking, but K48-linked ubiquitin chains are not. In contrast, depletion of K63-ubiquitin chains dramatically blocked CI-M6PR TGN localization and relocalized it to EEA1-positive endosomes (Figures 3F and S3G and data not shown), but had no significant effect on the overall organization of the TGN (Figure S3H). Similarly to the steady state behavior, retrograde transport of cell surface labeled CI-M6PR to the TGN is also dependent on K63-linked ubiquitination (Figures 3G and S3I). Furthermore, depletion of K63-linked ubiquitin chains altered trafficking of the lysosomal hydrolase Cathepsin D, resulting in the reduction of mature Cathepsin D, accumulation of pro- and intermediate-Cathepsin D, and the secretion of pro-Cathepsin D into the cell culture media (Figure 3H). These results suggest that K63-linked ubiquitination is important for proper retrograde transport.

MAGE-L2-TRIM27, Ube2O, and K63-Linked Ubiquitin Chains Are Required for Efficient Endosomal F-Actin Assembly

Next we assessed the precise mechanism by which MAGE-L2-TRIM27, Ube2O, and K63-linked ubiquitination promotes retrograde transport. Retrograde transport requires several ordered steps to facilitate endosome-to-Golgi transport, including endosomal localization of the Retromer complex and localization and activation of the SHRC to facilitate endosomal F-Actin accumulation by the Arp2/3 complex (Cullen and Korswagen, 2012). We interrogated several of these specific steps to determine when ubiquitination may be

important. The localization of the Retromer complex to CI-M6PR substrate containing endosomes was unaffected by depletion of TRIM27 or K63-linked ubiquitin chains (Figure S4A–B). In addition, the SHRC was still recruited normally to Retromer-positive endosomes in TRIM27-RNAi cells (Figure S4C). However, knockdown of MAGE-L2 or TRIM27 resulted in reduced endosomal F-Actin to a degree similar to WASH-RNAi (Figure 4A–B). Similarly, knockdown of the physiologically relevant Ube2O E2 enzyme, but not Ube2L6, resulted in a reduced endosomal F-actin (Figure 4A–B). Consistent with reduced endosomal F-actin, knockdown of MAGE-L2, TRIM27, or Ube2O, but not Ube2L6, significantly reduced the accumulation of the Arp2/3 complex subunit, ARPC5, on SHRC-positive endosomes (Figure 4C–D). Notably, there was no defect in total ARPC5 or F-actin levels (Figure 4D and data not shown). Likewise, depletion of K63-linked ubiquitin chains resulted in the specific reduction of endosomal F-actin and Arp2/3 complex, without affecting total F-actin, Arp2/3 complex, or SHRC levels (Figures 4E–4H, S3J, and data not shown). Consistent with the previously described role of SHRC and endosomal F-actin in membrane tubule scission (Derivery et al., 2009; Gomez and Billadeau, 2009), TRIM27-RNAi, shUb-Ub, and shUb-Ub(K63R) cells accumulated endosomal tubules (Figure S4D–E). These results suggest that K63-linked ubiquitination by MAGE-L2-TRIM27 and Ube2O is required for localization of the Arp2/3 complex to the SHRC and generation of endosomal F-Actin.

Uninhibited Endosomal Actin Assembly Rescues Endosome-to-Golgi Transport Defects of TRIM27-RNAi and K63-Ubiquitin Depleted Cells

We next examined whether the defective endosome-to-Golgi retrograde trafficking in TRIM27-RNAi or shUb-Ub(K63R) cells is due to decreased endosomal F-actin. First, we designed a fusion protein in which endosomal F-actin accumulation could be induced by an uninhibited WASH VCA motif. WASH VCA motif was fused to the C-terminal domain of FAM21 (Δ356N), which binds VPS35 for endosomal targeting (Figure 5A) (Gomez and Billadeau, 2009; Jia et al., 2012). Upon expression in cells, this fusion protein localized to Retromer-positive endosomes (Figure 5A) and increased F-Actin accumulation on endosomes (Figure 5A–B). We next determined whether this FAM21-WASH-VCA fusion could rescue retrograde transport in TRIM27-RNAi cells. Indeed this was the case for both Cathepsin D trafficking (Figure 5C) and CI-M6PR TGN localization (Figures 5D and S4F). Furthermore, the FAM21-WASH-VCA fusion rescued CI-M6PR trafficking in cells deficient for K63-linked ubiquitin chains (Figures 5E and S4G). Therefore, the primary requirement for TRIM27 and K63-linked ubiquitin chains in retrograde trafficking appears to be for accumulation of endosomal F-actin.

MAGE-L2-TRIM27 Ubiquitinates WASH K220 to Promote Endosomal F-Actin Assembly

Generation of endosomal F-Actin is facilitated by the SHRC, which binds the Arp2/3 complex and actin through a conserved VCA domain in WASH (Derivery et al., 2009; Gomez and Billadeau, 2009). However, the WASH VCA domain exists in an autoinhibited state that must be relieved before nucleation of F-actin by the Arp2/3 complex can be achieved (Jia et al., 2010). Therefore, we speculated that MAGE-L2-TRIM27 may facilitate WASH-VCA exposure, Arp2/3 complex and actin binding, and consequent F-Actin nucleation on endosomes through targeted ubiquitination of the SHRC. Based on the highly homologous WAVE regulatory complex, regulators of SHRC activation are predicted to act on WASH itself or SWIP (Chen et al., 2010; Jia et al., 2010). Although we were unable to detect any ubiquitination of endogenous SWIP (Figure S5A), endogenous WASH was highly ubiquitinated (Figure 6A). WASH ubiquitination was TRIM27-dependent, as knockdown of TRIM27 dramatically reduced endogenous WASH ubiquitination (Figure 6B). Furthermore, WASH ubiquitination was K63-linked, as WASH was unable to be

polyubiquitinated by K63R ubiquitin (Figure 6C). These findings suggest that TRIM27 is required for K63-linked ubiquitination of WASH.

Next we investigated the importance of WASH ubiquitination. To do so, we first determined the specific lysine in WASH that is conjugated to K63-linked ubiquitin chains. A single lysine, K220, in WASH had been identified in global proteomics studies to be ubiquitinated (Kim et al., 2011). Significantly, K220 is a highly conserved residue in species that express TRIM27 orthologues (Figure S5D). This residue is located in a region of WASH that is analogous to the “meander” region of WAVE, which is known to make contacts necessary for intra-complex inhibition in the WAVE regulatory complex (Chen et al., 2010). Therefore, we examined whether WASH ubiquitination was dependent on K220. Endogenous WASH was knocked down by RNAi and YFP-tagged wild-type or K220R WASH was re-expressed to insure integration of the re-expressed WASH into the SHRC. Unlike YFP-WASH wild-type, YFP-WASH K220R failed to be ubiquitinated (Figure 6C), suggesting that WASH ubiquitination is dependent on K220. We next examined whether WASH ubiquitination is important for retrograde transport. Using our re-expression system, YFP-WASH K220R, unlike wild-type YFP-WASH, could not support proper retrograde transport resulting in CI-M6PR dispersion (Figures 6D and S5B) and degradation (Figures 6E and S5B) and Cathepsin D secretion (Figure 6F). These results suggest that K63-linked ubiquitination of WASH K220 by TRIM27 is required for WASH function in retrograde transport.

We next examined whether WASH K220 ubiquitination may act as a signal to relieve WASH autoinhibition and promote its activity towards the Arp2/3 complex. As previously reported (Derivery et al., 2009), knockdown of WASH resulted in reduced endosomal Arp2/3 complex localization (Figures 6G and S5C). Unlike wild-type YFP-WASH, re-expression of YFP-WASH K220R was unable to rescue proper endosomal Arp2/3 complex localization (Figures 6G and S5C). Importantly, YFP-WASH K220R localized properly to endosomes indicating that it still incorporated into the SHRC (Figure S5C). These results suggest that ubiquitination of WASH K220 is required for WASH activation and Arp2/3 complex endosomal localization.

In vitro Reconstitution of MAGE-L2-TRIM27 and K63-Ubiquitin-Dependent SHRC Activity

Finally, we developed an in vitro reconstitution system to directly test whether ubiquitination of WASH is required for its actin assembling activity. To do so, we reconstituted WASH knockout MEFs (Gomez et al., 2012) with stable expression of HA-GFP-WASH wild-type, ΔVCA, or K220R. The intact SHRC was then purified from each of these cell lines by anti-HA chromatography to near homogeneity (Figure S6A–B). Under these conditions, very little free WASH is present (Figure S6B). The activity of the reconstituted SHRCs was first assayed by examining their capacity to assemble F-actin on beads in cell lysates (Cory et al., 2003). As expected, SHRC stimulated F-actin accumulation on beads in a manner dependent on the VCA motif of WASH and was inhibited by cytochalasin D (Figure 7A). Importantly, WASH knockout MEFs reconstituted with WASH K220R mutant did not support actin assembly on beads (Figure 7A). In addition, the activity of SHRC was dependent on MAGE-L2-TRIM27, as SHRC isolated from MAGE-L2- or TRIM27-RNAi cells was significantly less active (Figure 7B). Furthermore, we examined the activity of purified SHRC in Arp2/3 complex-dependent pyrene-actin assembly assays. SHRC reconstituted with wild-type, ubiquitinated WASH displayed increased activity toward the Arp2/3 complex compared to SHRC reconstituted with non-ubiquitinated WASH K220R (Figure 7C). To further examine the interplay of WASH ubiquitination and activity, we treated purified wild-type SHRC with the K63-specific deubiquitinating enzyme AMSH. This treatment deconjugated K63-ubiquitin chains from WASH (Figure 7D) and significantly inhibited SHRC activity on beads (Figure 7E)

and in pyrene-actin assembly assays (Figure 7F). These results suggest that K63-ubiquitination of WASH K220 by MAGE-L2-TRIM27 facilitates the activation of SHRC in a reversible manner.

To determine if ubiquitination of WASH K220 may facilitate SHRC activation by disrupting autoinhibitory contacts in the meander region around WASH K220, we mutated WASH K220 to aspartic acid (K220D) to destabilize autoinhibitory contacts in this region. Unlike inactive WASH K220R, WASH K220D is active in vitro (Figure 7A and 7C) and facilitates endosome-to-Golgi retrograde transport (Figure 6D–F) and endosomal Arp2/3 complex localization (Figure 6G) in cells. These results suggest that destabilizing the WASH meander region around the ubiquitination site can facilitate SHRC activity independent of ubiquitination.

DISCUSSION

MAGE proteins are a family of proteins that contain a conserved domain known as the MAGE homology domain. Recently, we showed that MAGE proteins function biochemically to bind to and enhance the activity of E3 RING ubiquitin ligases (Doyle et al., 2010). In this study we investigated the cellular function of one specific MAGE protein, MAGE-L2. Proteomic analysis revealed that MAGE-L2 specifically bound the TRIM27 E3 RING ubiquitin ligase. TRIM27 belongs to a large family of E3 RING ubiquitin ligases known as tripartite motif (TRIM) proteins. TRIM27 was originally identified and named Ret finger protein (RFP), due to its discovery as a gene that undergoes a translocation event with the Ret tyrosine kinase receptor in thyroid carcinomas (Saenko et al., 2003; Takahashi and Cooper, 1987). Subsequent work has implicated it in several processes, including transcriptional regulation, NFκB signaling, CD4+ T-cell homeostasis, and as an oncogene (Cai et al., 2011; Krutzfeldt et al., 2005; Shimono et al., 2000; Zha et al., 2006; Zoumpoulidou et al., 2012). It will be of particular interest in the future to determine if any of these diverse functions of TRIM27 are attributed to its regulation of WASH and vesicular transport.

Cellular studies revealed that MAGE-L2 and TRIM27 colocalized on cytoplasmic structures that were determined to be Retromer-positive endosomes. Of note, TRIM27 was previously shown to localize to similar structures that were unidentified at the time (Harbers et al., 2001). Furthermore, the localization of TRIM27 was regulated by PKC, JNK and RAS signaling pathways. To determine if any of these signaling pathways may contribute to the upstream regulation of MAGE-L2-TRIM27 and endosome-to-Golgi retrograde transport, we examined the effects of short-term inhibition of the PKC, JNK, MEK, and PI3K signaling pathways on the kinetics of surface CI-M6PR trafficking to the TGN. Specific inhibition of the JNK signaling pathway blocked CI-M6PR retrieval to the TGN (Figure S7). Future studies into the mechanism by which JNK signaling regulates endosomal protein recycling will be of particular interest.

Our mechanistic studies uncovered that K63-linked ubiquitination of WASH K220 by MAGE-L2-TRIM27 is required for endosomal F-actin nucleation and retrograde transport. WASH K220 is predicted to exist in an analogous region on the SHRC as the meander region on the known WAVE regulatory complex structure. The meander region makes contacts with WAVE itself and SRA1 (analogous to SWIP in SHRC) and is essential for maintaining WAVE in an inactive state (Chen et al., 2010). Importantly, this region is subjected to regulation by phosphorylation (Padrick and Rosen, 2010). Thus, the proposed meander region on both the WAVE and WASH regulatory complexes may be regulated by post-translational modifications, phosphorylation and ubiquitination, respectively. In addition, WASH K220 is highly conserved in vertebrates where TRIM27 is found.

However, it is not conserved in invertebrates where TRIM27 orthologs are not present (Boudinot et al., 2011). Thus, regulation of SHRC by ubiquitination is likely highly conserved in vertebrates, but additional forms of regulation are predicted in invertebrates.

Our results suggest that ubiquitination of WASH facilitates activation by directly destabilizing autoinhibitory contacts in the SHRC, thus allowing VCA exposure, Arp2/3 complex binding, and subsequent F-actin assembly (Figure 7G). Consistently, destabilizing these autoinhibitory contacts bypasses the requirement for WASH ubiquitination. In the context of the cell, other factors likely cooperate to further enhance activity, perhaps by clustering the active SHRC. Another likely point of regulation is in deactivating WASH after sufficient endosomal F-actin nucleation for retrograde trafficking. Indeed, we find that ubiquitin-mediated activation of SHRC is reversible. Future studies into relevant deubiquitinating enzymes will be of interest.

Our findings also provide important insights into pathological conditions associated with MAGE-L2, TRIM27, and retrograde transport. Genes required for retrograde transport are frequently amplified in melanomas, contribute to tumorigenesis, and mediate trafficking of proteins required for tumor progression (Scott et al., 2009; Zech et al., 2011). Our findings extend this work to show that the TRIM27 oncogene facilitates integrin α5 recycling, an important event in tumorigenesis. Additionally, retrograde transport has been implicated in Alzheimer's disease, where components of the pathway are downregulated and mutated (Small, 2008). Similarly, MAGE-L2 has been reported to be downregulated in the hippocampus of patients with incipient Alzheimer's disease (Blalock et al., 2004). Finally, retrograde transport is an essential pathway in which many microbial toxins and some viruses enter cells. Indeed, inhibition of TRIM27 blocks trafficking of cholera toxin. Our results suggest a novel potential strategy to combat these pathogens.

EXPERIMENTAL PROCEDURES

Cell Culture, Transfections, siRNAs, and Antibodies

Cells were cultured under standard conditions and transfected according to manufacturer's recommendation. Detailed descriptions of cell culture conditions, transfection procedures, siRNA sequences, and antibodies are described in the Extended Experimental Procedures.

Tandem Affinity Purification and Mass Spectrometry

Tandem affinity purification (TAP) was performed using 293/TAP-Vector or 293/TAP-MAGE-L2 stable cell lines as described previously (Doyle et al., 2010) and in the Extended Experimental Procedures.

Immunoprecipitation, Immunoblotting, and Cathepsin D Secretion Assay

Immunoprecipitation and immunoblotting were performed as described previously (Potts and Yu, 2005). Cathepsin D secretion assay details are described in the Extended Experimental Procedures.

Protein Purification and In Vitro Binding Assays

Recombinant proteins were produced using standard procedures described in the Extended Experimental Procedures. In vitro binding assays were performed as described previously (Doyle et al., 2010) and specified in the Extended Experimental Procedures.

Immunofluorescence, Microscopy, and Quantitative Measurements

Immunofluorescence was performed essentially as described previously (Potts and Yu, 2007) and in Extended Experimental Procedures. Retrograde transport of cell surface CI-M6PR was performed as described previously (Gomez and Billadeau, 2009) and detailed in the Extended Experimental Procedures.

Actin Assembly Assays and Purification of SHRC

WASH knockout MEFs (Gomez et al., 2012) were reconstituted with HA-GFP-tagged WASH and the resulting SHRC variants were purified as described in the Extended Experimental Procedures. Bead based and pyrene-actin assembly assays were performed as described previously (Cory et al., 2003; Jia et al., 2010) and detailed in the Extended Experimental Procedures.

Supplementary Material

Refer to Web version on PubMed Central for supplementary material.

Acknowledgments

We thank Mitsuaki Tabuchi (Kawasaki Medical School, Japan) for providing the Retromer construct. We also thank Potts lab members for helpful discussions and critical reading of the manuscript. This work was supported by the Sara and Frank McKnight Fellowship (PRP), Michael L. Rosenberg Scholar in Medical Research fund (PRP), Cancer Prevention and Research Initiative of Texas R1117 (PRP), the Mayo Foundation and National Institutes of Health Grant R01-AI065474 (DDB).

References

Arighi CN, Hartnell LM, Aguilar RC, Haft CR, Bonifacino JS. Role of the mammalian retromer in sorting of the cation-independent mannose 6-phosphate receptor. J Cell Biol. 2004; 165:123–133. [PubMed: 15078903]

Bischof JM, Stewart CL, Wevrick R. Inactivation of the mouse Magel2 gene results in growth abnormalities similar to Prader-Willi syndrome. Hum Mol Genet. 2007; 16:2713–2719. [PubMed: 17728320]

Blalock EM, Geddes JW, Chen KC, Porter NM, Markesbery WR, Landfield PW. Incipient Alzheimer's disease: microarray correlation analyses reveal major transcriptional and tumor suppressor responses. Proc Natl Acad Sci U S A. 2004; 101:2173–2178. [PubMed: 14769913]

Boccaccio I, Glatt-Deeley H, Watrin F, Roeckel N, Lalande M, Muscatelli F. The human MAGEL2 gene and its mouse homologue are paternally expressed and mapped to the Prader-Willi region. Hum Mol Genet. 1999; 8:2497–2505. [PubMed: 10556298]

Bochtler M, Ditzel L, Groll M, Hartmann C, Huber R. The proteasome. Annu Rev Biophys Biomol Struct. 1999; 28:295–317. [PubMed: 10410804]

Bonifacino JS, Hurley JH. Retromer. Curr Opin Cell Biol. 2008; 20:427–436. [PubMed: 18472259]

Bonifacino JS, Rojas R. Retrograde transport from endosomes to the trans-Golgi network. Nat Rev Mol Cell Biol. 2006; 7:568–579. [PubMed: 16936697]

Boudinot P, van der Aa LM, Jouneau L, Du Pasquier L, Pontarotti P, Briolat V, Benmansour A, Levraud JP. Origin and evolution of TRIM proteins: new insights from the complete TRIM repertoire of zebrafish and pufferfish. PLoS One. 2011; 6:e22022. [PubMed: 21789205]

Brass AL, Dykxhoorn DM, Benita Y, Yan N, Engelman A, Xavier RJ, Lieberman J, Elledge SJ. Identification of host proteins required for HIV infection through a functional genomic screen. Science. 2008; 319:921–926. [PubMed: 18187620]

Cai X, Srivastava S, Sun Y, Li Z, Wu H, Zuvela-Jelaska L, Li J, Salamon RS, Backer JM, Skolnik EY. Tripartite motif containing protein 27 negatively regulates CD4 T cells by ubiquitinating and inhibiting the class II PI3K-C2beta. Proc Natl Acad Sci U S A. 2011; 108:20072–20077. [PubMed: 22128329]

Campellone KG, Welch MD. A nucleator arms race: cellular control of actin assembly. Nat Rev Mol Cell Biol. 2010; 11:237–251. [PubMed: 20237478]

Chen Z, Borek D, Padrick SB, Gomez TS, Metlagel Z, Ismail AM, Umetani J, Billadeau DD, Otwinowski Z, Rosen MK. Structure and control of the actin regulatory WAVE complex. Nature. 2010; 468:533–538. [PubMed: 21107423]

Chomez P, De Backer O, Bertrand M, De Plaen E, Boon T, Lucas S. An overview of the MAGE gene family with the identification of all human members of the family. Cancer Res. 2001; 61:5544–5551. [PubMed: 11454705]

Cory GO, Cramer R, Blanchoin L, Ridley AJ. Phosphorylation of the WASP-VCA domain increases its affinity for the Arp2/3 complex and enhances actin polymerization by WASP. Mol Cell. 2003; 11:1229–1239. [PubMed: 12769847]

Cullen PJ, Korswagen HC. Sorting nexins provide diversity for retromer-dependent trafficking events. Nat Cell Biol. 2012; 14:29–37. [PubMed: 22193161]

Derivery E, Sousa C, Gautier JJ, Lombard B, Loew D, Gautreau A. The Arp2/3 activator WASH controls the fission of endosomes through a large multiprotein complex. Dev Cell. 2009; 17:712–723. [PubMed: 19922875]

Doyle JM, Gao J, Wang J, Yang M, Potts PR. MAGE-RING protein complexes comprise a family of E3 ubiquitin ligases. Mol Cell. 2010; 39:963–974. [PubMed: 20864041]

Duleh SN, Welch MD. WASH and the Arp2/3 complex regulate endosome shape and trafficking. Cytoskeleton (Hoboken). 2010; 67:193–206. [PubMed: 20175130]

Duleh SN, Welch MD. Regulation of integrin trafficking, cell adhesion, and cell migration by WASH and the Arp2/3 complex. Cytoskeleton (Hoboken). 2012

Eden S, Rohatgi R, Podtelejnikov AV, Mann M, Kirschner MW. Mechanism of regulation of WAVE1-induced actin nucleation by Rac1 and Nck. Nature. 2002; 418:790–793. [PubMed: 12181570]

Fang S, Weissman AM. A field guide to ubiquitylation. Cell Mol Life Sci. 2004; 61:1546–1561. [PubMed: 15224180]

Gomez TS, Billadeau DD. A FAM21-containing WASH complex regulates retromer-dependent sorting. Dev Cell. 2009; 17:699–711. [PubMed: 19922874]

Gomez TS, Gorman JA, Artal-Martinez de Narvajas A, Koenig AO, Billadeau DD. Trafficking Defects in WASH Knockout Fibroblasts Originate from Collapsed Endosomal and Lysosomal Networks. Mol Biol Cell. 2012

Harbers M, Nomura T, Ohno S, Ishii S. Intracellular localization of the Ret finger protein depends on a functional nuclear export signal and protein kinase C activation. J Biol Chem. 2001; 276:48596–48607. [PubMed: 11591718]

Harbour ME, Breusegem SY, Seaman MN. Recruitment of the endosomal WASH complex is mediated by the extended ‘tail’ of Fam21 binding to the retromer protein Vps35. Biochem J. 2012; 442:209–220. [PubMed: 22070227]

Ismail AM, Padrick SB, Chen B, Umetani J, Rosen MK. The WAVE regulatory complex is inhibited. Nat Struct Mol Biol. 2009; 16:561–563. [PubMed: 19363480]

Jia D, Gomez TS, Billadeau DD, Rosen MK. Multiple repeat elements within the FAM21 tail link the WASH actin regulatory complex to the retromer. Mol Biol Cell. 2012; 23:2352–2361. [PubMed: 22513087]

Jia D, Gomez TS, Metlagel Z, Umetani J, Otwinowski Z, Rosen MK, Billadeau DD. WASH and WAVE actin regulators of the Wiskott-Aldrich syndrome protein (WASP) family are controlled by analogous structurally related complexes. Proceedings of the National Academy of Sciences of the United States of America. 2010; 107:10442–10447. [PubMed: 20498093]

Johannes L, Popoff V. Tracing the retrograde route in protein trafficking. Cell. 2008; 135:1175–1187. [PubMed: 19109890]

Kim AS, Kakalis LT, Abdul-Manan N, Liu GA, Rosen MK. Autoinhibition and activation mechanisms of the Wiskott-Aldrich syndrome protein. Nature. 2000; 404:151–158. [PubMed: 10724160]

Kim W, Bennett EJ, Huttlin EL, Guo A, Li J, Possemato A, Sowa ME, Rad R, Rush J, Comb MJ, et al. Systematic and quantitative assessment of the ubiquitin-modified proteome. Mol Cell. 2011; 44:325–340. [PubMed: 21906983]

Kozlov SV, Bogenpohl JW, Howell MP, Wevrick R, Panda S, Hogenesch JB, Muglia LJ, Van Gelder RN, Herzog ED, Stewart CL. The imprinted gene Magel2 regulates normal circadian output. Nat Genet. 2007; 39:1266–1272. [PubMed: 17893678]

Krutzfeldt M, Ellis M, Weekes DB, Bull JJ, Eilers M, Vivanco MD, Sellers WR, Mittnacht S. Selective ablation of retinoblastoma protein function by the RET finger protein. Mol Cell. 2005; 18:213–224. [PubMed: 15837424]

Lebensohn AM, Kirschner MW. Activation of the WAVE complex by coincident signals controls actin assembly. Mol Cell. 2009; 36:512–524. [PubMed: 19917258]

Linardopoulou EV, Parghi SS, Friedman C, Osborn GE, Parkhurst SM, Trask BJ. Human subtelomeric WASH genes encode a new subclass of the WASP family. PLoS Genet. 2007; 3:e237. [PubMed: 18159949]

Liu R, Abreu-Blanco MT, Barry KC, Linardopoulou EV, Osborn GE, Parkhurst SM. Wash functions downstream of Rho and links linear and branched actin nucleation factors. Development. 2009; 136:2849–2860. [PubMed: 19633175]

Markson G, Kiel C, Hyde R, Brown S, Charalabous P, Bremm A, Semple J, Woodsmith J, Duley S, Salehi-Ashtiani K, et al. Analysis of the human E2 ubiquitin conjugating enzyme protein interaction network. Genome Res. 2009; 19:1905–1911. [PubMed: 19549727]

Miki H, Sasaki T, Takai Y, Takenawa T. Induction of filopodium formation by a WASP-related actin-depolymerizing protein N-WASP. Nature. 1998; 391:93–96. [PubMed: 9422512]

Padrick SB, Rosen MK. Physical mechanisms of signal integration by WASP family proteins. Annu Rev Biochem. 2010; 79:707–735. [PubMed: 20533885]

Potts PR, Yu H. Human MMS21/NSE2 is a SUMO ligase required for DNA repair. Mol Cell Biol. 2005; 25:7021–7032. [PubMed: 16055714]

Potts PR, Yu H. The SMC5/6 complex maintains telomere length in ALT cancer cells through SUMOylation of telomere-binding proteins. Nat Struct Mol Biol. 2007; 14:581–590. [PubMed: 17589526]

Saenko V, Rogounovitch T, Shimizu-Yoshida Y, Abrosimov A, Lushnikov E, Roumiantsev P, Matsumoto N, Nakashima M, Meirmanov S, Ohtsuru A, et al. Novel tumorigenic rearrangement, Delta rfp/ret, in a papillary thyroid carcinoma from externally irradiated patient. Mutat Res. 2003; 527:81–90. [PubMed: 12787916]

Sandvig K, van Deurs B. Delivery into cells: lessons learned from plant and bacterial toxins. Gene Ther. 2005; 12:865–872. [PubMed: 15815697]

Scott KL, Kabbarah O, Liang MC, Ivanova E, Anagnostou V, Wu J, Dhakal S, Wu M, Chen S, Feinberg T, et al. GOLPH3 modulates mTOR signalling and rapamycin sensitivity in cancer. Nature. 2009; 459:1085–1090. [PubMed: 19553991]

Shimono Y, Murakami H, Hasegawa Y, Takahashi M. RET finger protein is a transcriptional repressor and interacts with enhancer of polycomb that has dual transcriptional functions. J Biol Chem. 2000; 275:39411–39419. [PubMed: 10976108]

Small SA. Retromer sorting: a pathogenic pathway in late-onset Alzheimer disease. Arch Neurol. 2008; 65:323–328. [PubMed: 18332244]

Sun L, Chen ZJ. The novel functions of ubiquitination in signaling. Curr Opin Cell Biol. 2004; 16:119–126. [PubMed: 15196553]

Takahashi M, Cooper GM. ret transforming gene encodes a fusion protein homologous to tyrosine kinases. Mol Cell Biol. 1987; 7:1378–1385. [PubMed: 3037315]

Tennese AA, Wevrick R. Impaired hypothalamic regulation of endocrine function and delayed counterregulatory response to hypoglycemia in Magel2-null mice. Endocrinology. 2011; 152:967–978. [PubMed: 21248145]

Xu M, Skaug B, Zeng W, Chen ZJ. A ubiquitin replacement strategy in human cells reveals distinct mechanisms of IKK activation by TNFalpha and IL-1beta. Mol Cell. 2009; 36:302–314. [PubMed: 19854138]

Zech T, Calaminus SD, Caswell P, Spence HJ, Carnell M, Insall RH, Norman J, Machesky LM. The Arp2/3 activator WASH regulates alpha5beta1-integrin-mediated invasive migration. J Cell Sci. 2011; 124:3753–3759. [PubMed: 22114305]

Zha J, Han KJ, Xu LG, He W, Zhou Q, Chen D, Zhai Z, Shu HB. The Ret finger protein inhibits signaling mediated by the noncanonical and canonical IkappaB kinase family members. J Immunol. 2006; 176:1072–1080. [PubMed: 16393995]

Zoumpoulidou G, Broceno C, Li H, Bird D, Thomas G, Mittnacht S. Role of the tripartite motif protein 27 in cancer development. J Natl Cancer Inst. 2012; 104:941–952. [PubMed: 22556269]

Highlights

- MAGE-L2-TRIM27 E3 ubiquitin ligase localizes to Retromer-positive endosomes
- Retrograde transport requires MAGE-L2-TRIM27, Ube2O, and K63-ubiquitination
- MAGE-L2-TRIM27, Ube2O, and K63-ubiquitination facilitate endosomal actin nucleation
- WASH is activated by K63-linked ubiquitination of WASH K220 by MAGE-L2-TRIM27

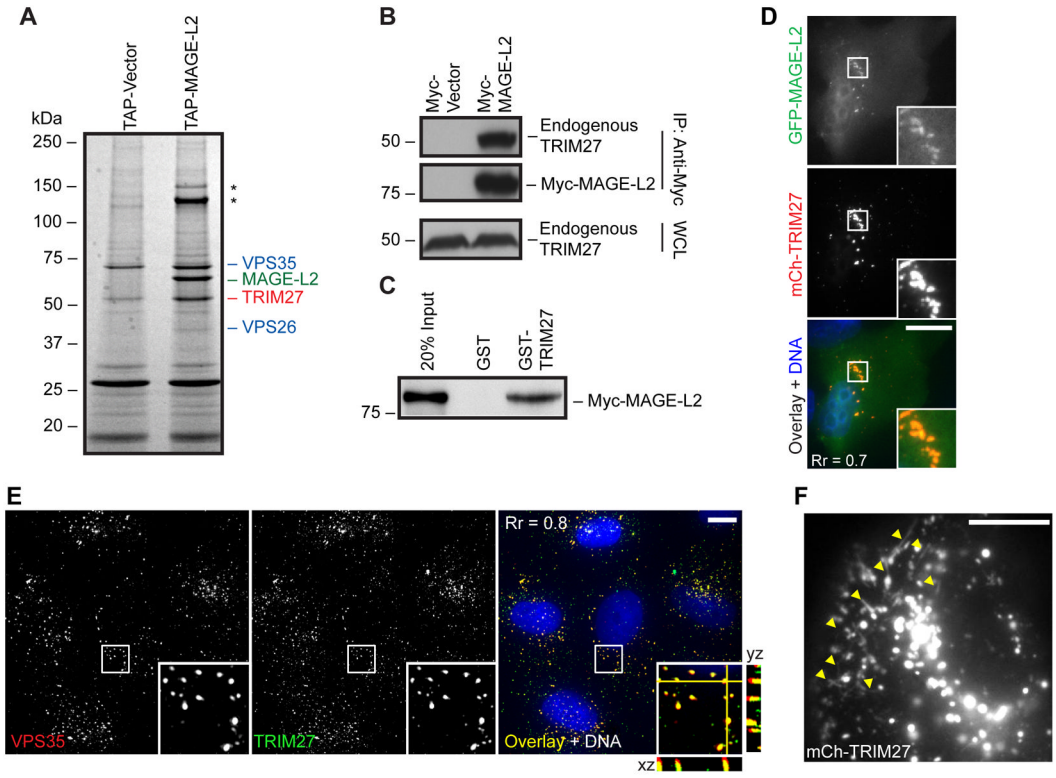

Figure 1. MAGE-L2 binds TRIM27 and localizes to Retromer-positive endosomes

(A) TAP-Vector or TAP-MAGE-L2 were isolated from HEK293 stable cell lines, separated by SDS-PAGE, coomassie stained, and the identity of specific bands was determined by LC-MS/MS. Asterisks indicate Usp7.

(B) The indicated proteins were expressed in cells for 48 hours, anti-Myc IP was performed, and proteins were detected by western blot (WB).

(C) Binding of Myc-MAGE-L2 to recombinant GST-TRIM27 or GST alone was determined by GST pull-down assays and anti-Myc immunoblotting.

(D) Stably expressed GFP-MAGE-L2 and mCherry-TRIM27 co-localize in specific cytoplasmic puncta.

(E) U2OS cells were stained for endogenous VPS35 (red), endogenous TRIM27 (green), and DNA (blue). XZ and YZ projection stacks are shown.

(F) Live cell imaging of stably expressed mCherry-TRIM27 shows localization to tubule-like protrusions (yellow arrowheads) from endosomes.

Pearson's correlation coefficients (Rr) are shown. All scale bars indicate 20 μm. See also Figure S1.

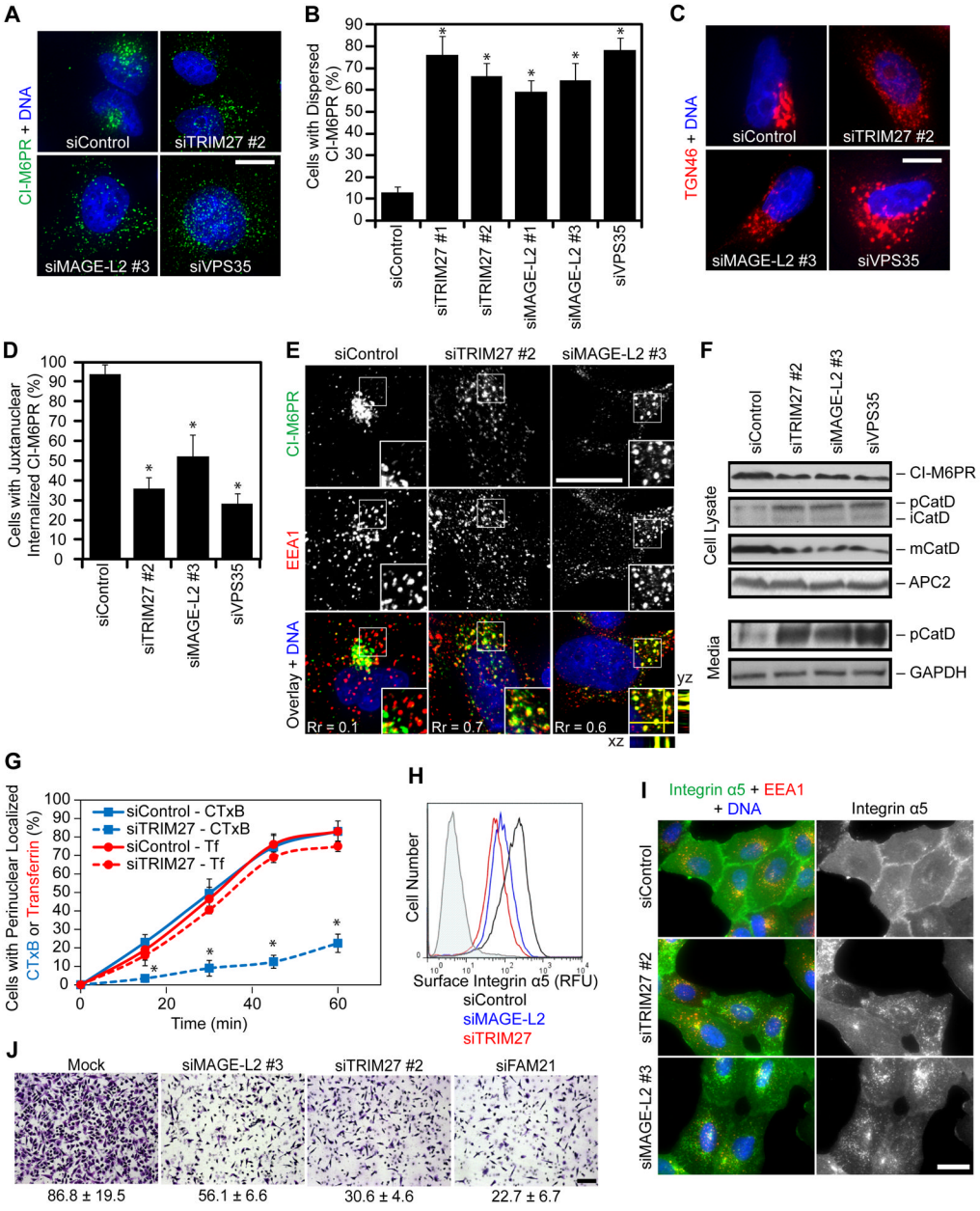

Figure 2. MAGE-L2-TRIM27 is required for endosomal protein recycling

(A) Cells were treated with the indicated siRNAs for 72 hours and stained for CI-M6PR (green) and DNA (blue).

(B) Quantitation of cells shown in (A). Compact juxtanuclear or dispersed CI-M6PR was scored and the percentage of cells with dispersed CI-M6PR is shown.

(C) Cells were treated with the indicated siRNAs for 72 hours and stained for TGN46 (red) and DNA (blue).

(D) Cells were treated with the indicated siRNAs. Cell surface CI-M6PR was labeled with anti-CI-M6PR antibody for one hour before imaging the pool of internalized cell surface-labeled CI-M6PR.

(E) Cells were treated with the indicated siRNAs and stained for CI-M6PR (green), EEA1 (red) and DNA (blue). XZ and YZ projection stacks and Pearson's correlation coefficients (Rr) are shown.
(F) Cells were treated with the indicated siRNAs for 72 hours and cell lysates and media were analyzed by immunoblotting. pCatD represents unprocessed pro-CatD, iCatD indicates intermediate processed CatD, and mCatD represents fully matured CatD.
(G) Cells were treated with the indicated siRNAs for 72 hours and transport of CTxB-488 or Tf-568 was determined at the indicated times.
(H) Cells were treated with the indicated siRNAs for 72 hours and surface integrin α5 was determined by flow cytometry. Grey curve indicates control IgG staining.
(I) Cells were treated with the indicated siRNAs for 72 hours and immunostained with integrin α5 (green), EEA1 (red), and DNA (blue).
(J) Invasive potential of cells treated with the indicated siRNAs was assayed on matrigel-coated transwell invasion chambers. Invaded cells were stained with crystal violet and quantitated.
All data are represented as the mean +SD. Asterisk indicates $p<0.05$. All scale bars indicate 20 μm. See also Figure S2 and S7.

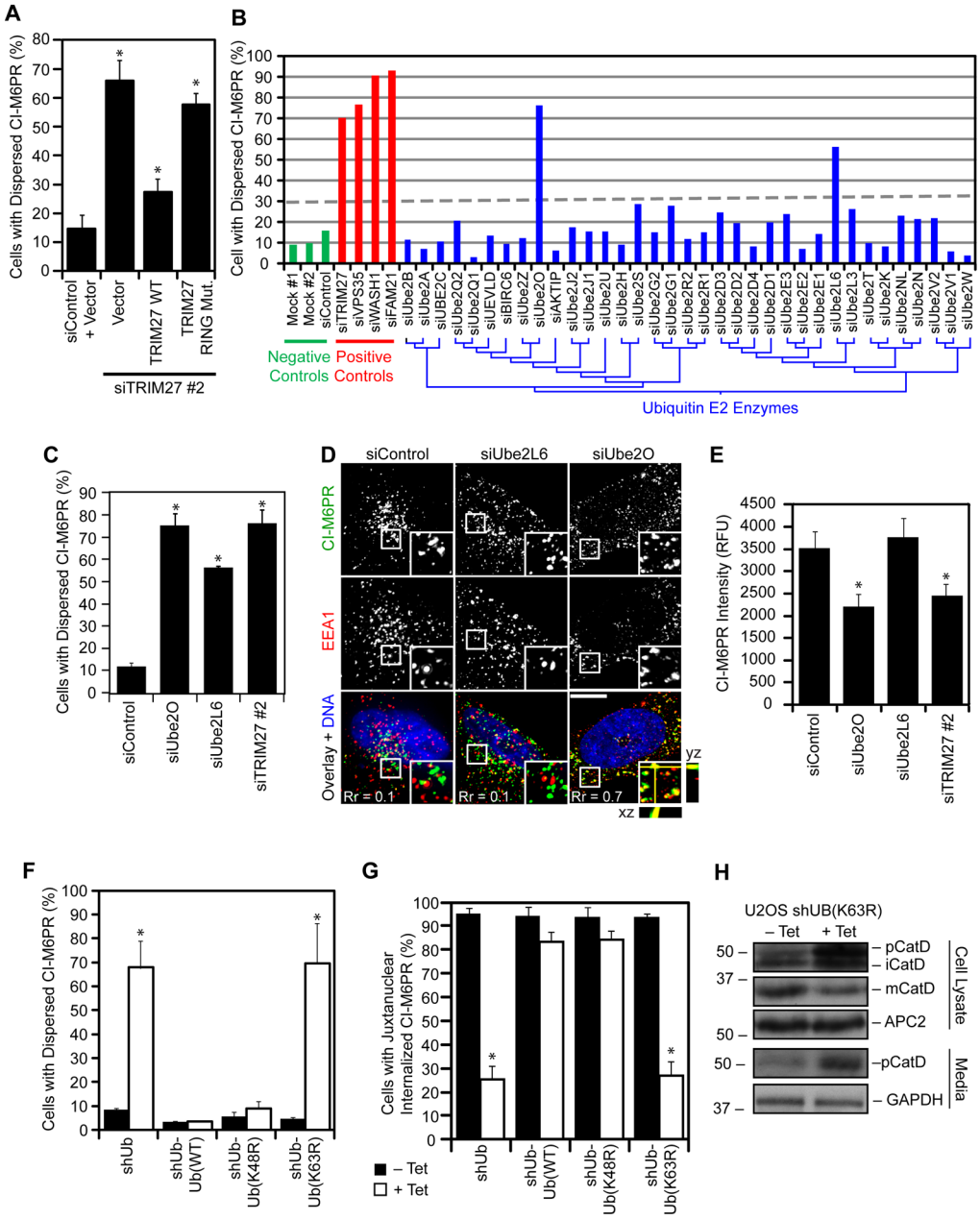

Figure 3. Ube2O E2 and K63-ubiquitin chains are required for retrograde transport

(A) Cells were treated with control or TRIM27 siRNAs for 24 hours before transfection of RNAi-resistant wild-type or RING mutant TRIM27. Forty-eight hours after transfection, cells were stained for CI-M6PR. The percentage of transfected cells with dispersed CI-M6PR is shown.

(B) Cells were treated with siRNAs targeting the indicated E2 enzymes for 72 hours, stained with anti-CI-M6PR, imaged, and quantitated. Dotted line denotes cutoff that reproducibly indicates CI-M6PR trafficking defect.

(C) Cells were treated with the indicated siRNAs for 72 hours, stained with CI-M6PR, and imaged. The percentage of cells with dispersed CI-M6PR is shown.

(D) Cells were treated with the indicated siRNAs for 72 hours and stained for CI-M6PR (green), EEA1 (red) and DNA (blue). XZ and YZ projection stacks and Pearson's correlation coefficients (Rr) are shown.
(E) Cells were treated with the indicated siRNAs for 72 hours, stained for CI-M6PR, imaged, and CI-M6PR intensity was determined.
(F) Ubiquitin replacement cell lines were treated with or without tetracycline for 72–96 hours before steady-state CI-M6PR localization was determined by immunostaining. The percentage of cells with dispersed CI-M6PR is shown.
(G) Ubiquitin replacement cells were treated with or without tetracycline for 72–96 hours. Cell surface CI-M6PR was then labeled with anti-CI-M6PR antibody for one hour and internalized cell surface-labeled CI-M6PR was imaged. CI-M6PR localization was determined and the percentage of cells showing juxtanuclear internalized CI-M6PR is shown.
(H) Cells were treated with the indicated siRNAs for 72 hours before Cathepsin D processing and secretion was determined by immunoblotting. pCatD represents unprocessed pro-CatD, iCatD indicates intermediate processed CatD, and mCatD represents fully matured CatD.
Data are represented as the mean +SD. Asterisk indicates $p<0.05$. All scale bars indicate 20 μm. See also Figure S3.

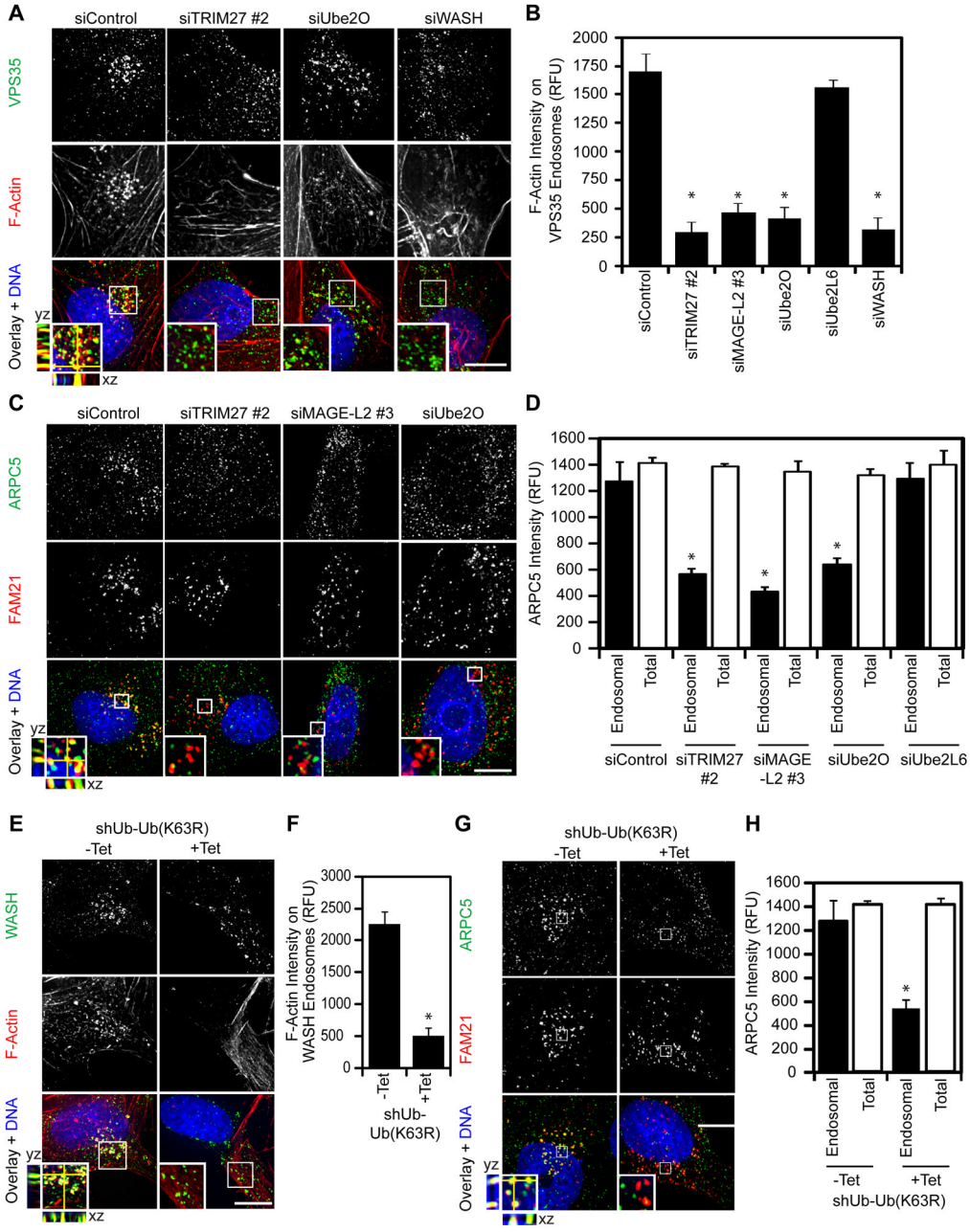

Figure 4. MAGE-L2-TRIM27, Ube2O, and K63-linked ubiquitination are required for endosomal F-actin assembly

(A) Cells were treated with the indicated siRNAs for 72 hours before staining VPS35 (green), F-Actin (red), and DNA (blue). XZ and YZ projection stacks are shown.

(B) F-Actin intensity on VPS35-positive endosomes of cells described in (A).

(C) Cells were treated with the indicated siRNAs for 72 hours before staining ARPC5 (green), FAM21 (red), and DNA (blue). XZ and YZ projection stacks are shown.

(D) Cells treated as in (C) were imaged and endosomal (solid bars) or total (open bars) ARPC5 levels were determined.

(E) shUb-Ub(K63R) ubiquitin replacement cells were treated with or without tetracycline for 96 hours before staining for WASH (green), F-Actin (red), and DNA (blue). XZ and YZ projection stacks are shown.
(F) Cells described in (E) were imaged and F-actin intensity on Retromer-positive endosomes was quantitated and is shown.
(G) shUb-Ub(K63R) ubiquitin replacement cells were treated with or without tetracycline for 96 hours before staining with ARPC5 (green), FAM21 (red), and DNA (blue). XZ and YZ projection stacks are shown.
(H) Cells treated as in (G) were imaged and endosomal (solid bars) or total (open bars) ARPC5 levels were determined.
Data are represented as the mean +SD. Asterisk indicates $p<0.05$. All scale bars indicate 20 μm. See also Figure S4.

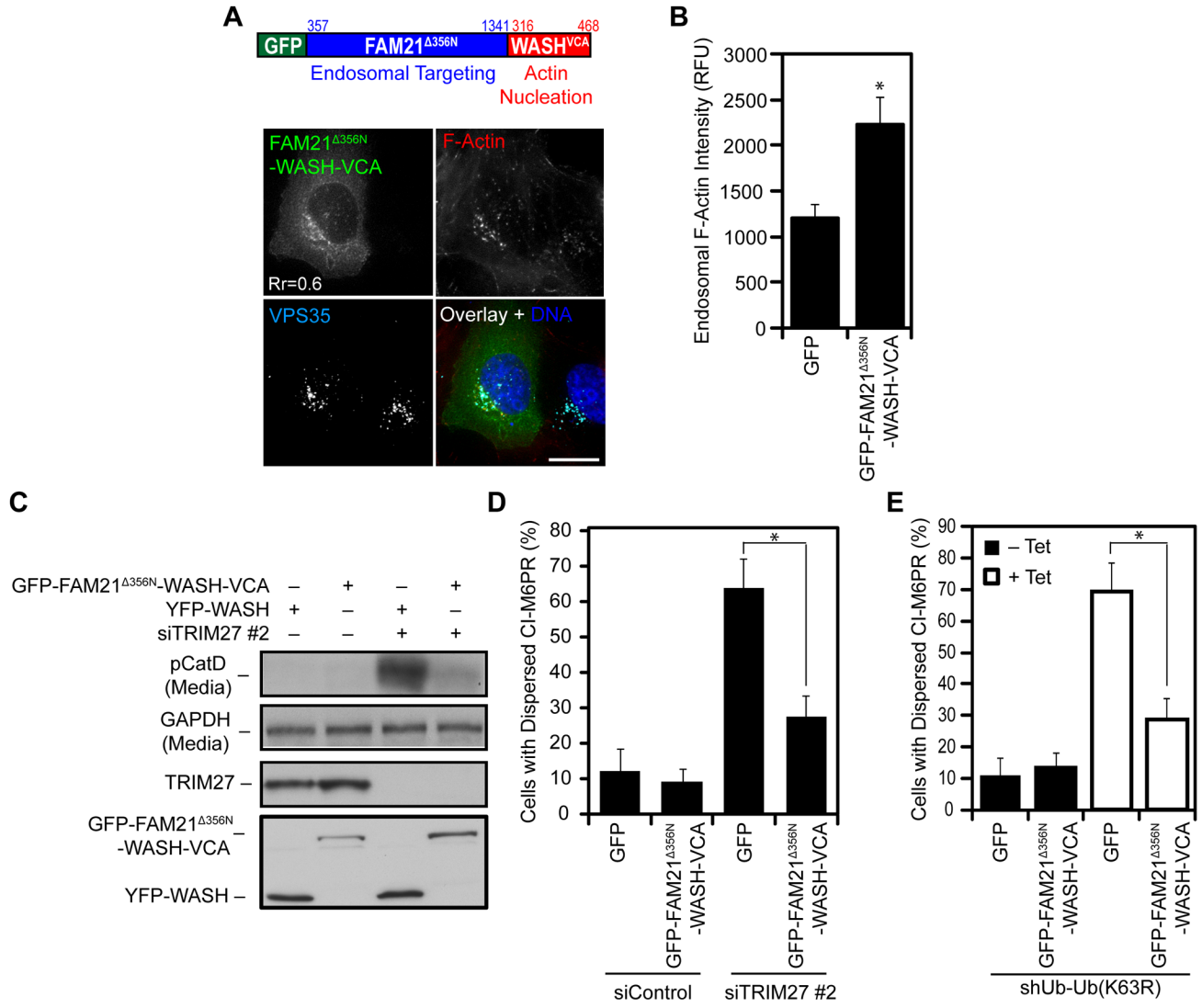

Figure 5. Uninhibited WASH-VCA bypasses the requirement for TRIM27 and K63-linked ubiquitin chains in retrograde transport

(A) Schematic of uninhibited, endosomal localized WASH-VCA (top). Cells were transiently transfected for 48 hours before staining GFP-FAM21$^{\Delta 356N}$-WASH-VCA (green), F-actin (red), VPS35 (cyan), and DNA (blue). Scale bar indicates 20 μm. Pearson's correlation coefficient (Rr) is shown.

(B) Cells were transfected with GFP-alone or GFP-FAM21$^{\Delta 356N}$-WASH-VCA and VPS35-localized F-Actin intensity was determined.

(C) Cells were treated with control or TRIM27 siRNAs for 24 hours before transfection with control YFP-WASH or constitutively active GFP-FAM21$^{\Delta 356N}$-WASH-VCA. Forty-eight hours later, the indicated proteins were examined by immunoblotting.

(D) Cells were treated with control or TRIM27 siRNAs for 24 hours before transfection with GFP alone or GFP-FAM21$^{\Delta 356N}$-WASH-VCA. Forty-eight hours after transfection, cells were immunostained for CI-M6PR and the percentage of transfected cells with dispersed CI-M6PR was determined.

(E) shUb-Ub(K63R) cells were treated with or without tetracycline and transfected with either GFP alone or GFP-FAM21$^{\Delta 356N}$-WASH-VCA. Cells were immunostained after 96

hours for CI-M6PR and the percentage of transfected cells with dispersed CI-M6PR was determined.

Data are represented as the mean +SD. Asterisk indicates $p<0.05$.

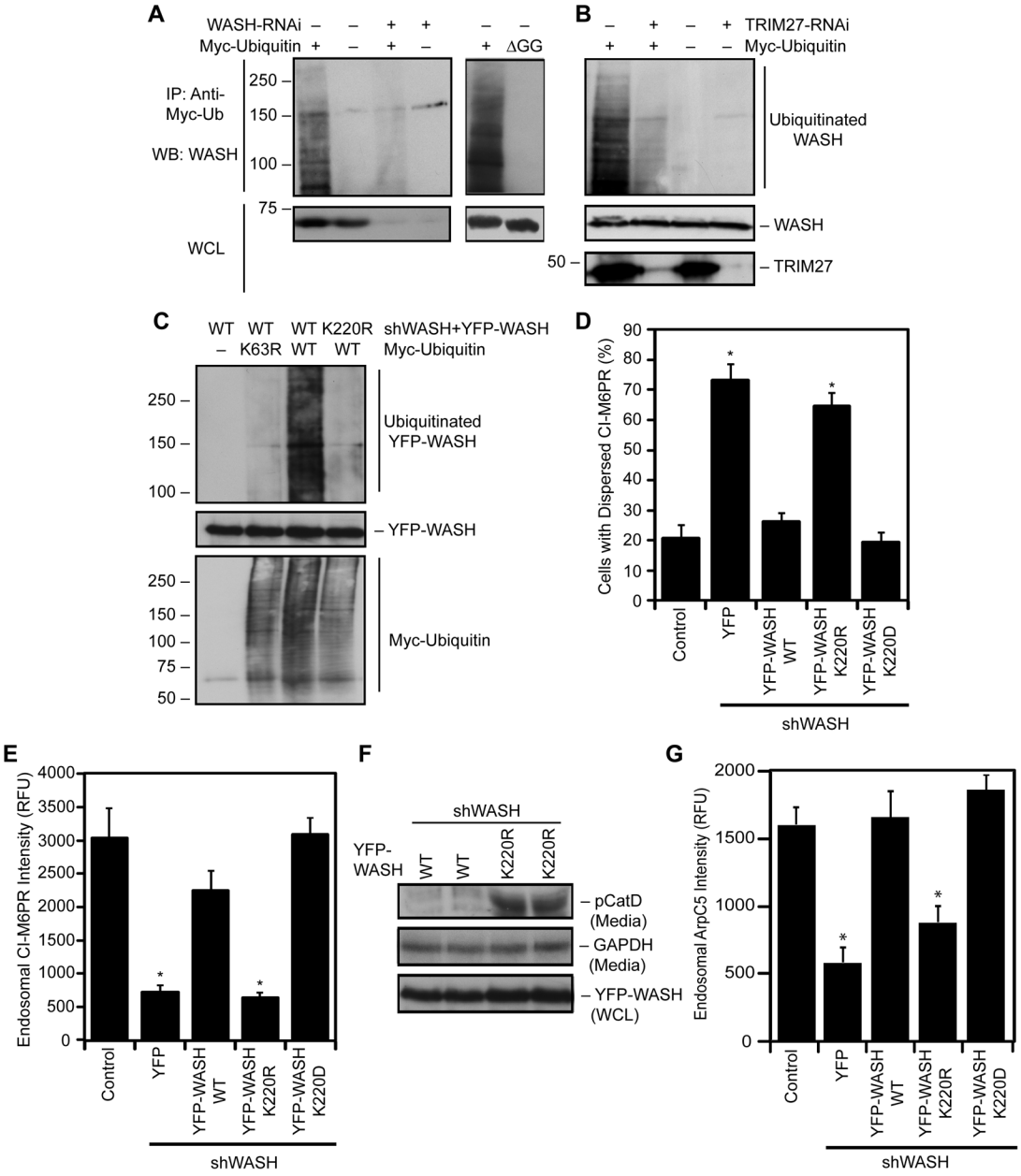

Figure 6. WASH K63-linked ubiquitination by TRIM27 is required for endosomal F-actin nucleation and retrograde transport

(A–B) Cells were treated with the indicated siRNAs for 24 hours before transfection of the indicated vectors. Forty-eight hours after plasmid transfection, anti-Myc IP was performed. Whole cell lysates (WCL) or anti-Myc IP samples were immunoblotted for WASH and TRIM27.

(C) Cells were transfected with the indicated Myc-ubiquitin vectors and dual-knockdown/re-expression vectors to knockdown endogenous WASH and re-express YFP-wild-type or K220R WASH. Seventy-two hours after transfection, anti-Myc IP was performed. Whole cell lysates (WCL) or anti-Myc IP samples were immunoblotted for WASH and Myc-ubiquitin.

(D–E) Cells were transfected with the indicated dual-knockdown/re-expression vectors to knockdown endogenous WASH and re-express YFP-WASH variants. Seventy-two hours after transfection cells were immunostained for CI-M6PR and dispersed CI-M6PR (D) and endosomal CI-M6PR abundance (E) was determined in transfected cells.
(F) Cells were transfected with the indicated dual-knockdown/re-expression vectors as indicated. Seventy-two hours after transfection Cathepsin D secretion into the cell culture media was determined by immunoblotting. Two independent samples from each condition are shown.
(G) Cells described in (D) were immunostained for ARPC5 and the endosomal-localized pool of ARPC5 in transfected cells was quantitated.
Data are represented as the mean +SD. Asterisk indicates $p<0.05$. See also Figure S5.

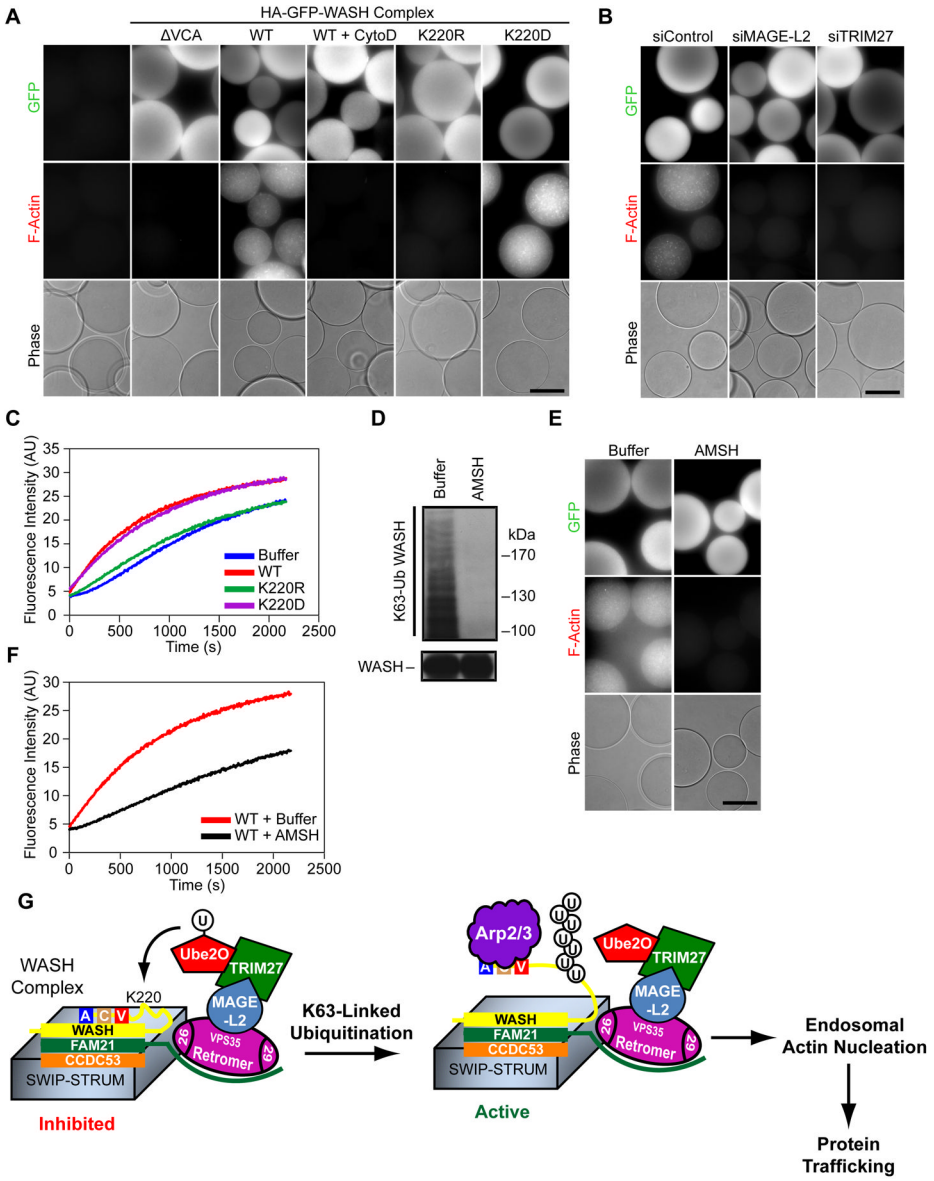

Figure 7. In vitro Reconstitution of MAGE-L2-TRIM27 and K63-ubiquitin-dependent SHRC activity

(A) Cell lysates from WASH knockout MEFs reconstituted with the indicated HA-GFP-WASH proteins were incubated with anti-HA agarose beads and F-actin stained with phalloidin-568. WT+CytoD was treated with 10 μM cytochalasin D before addition of beads.

(B) WASH knockout MEFs reconstituted with wild-type HA-GFP-WASH were transfected with the indicated siRNAs for 96 hours and actin assembly was determined as described in (A).

(C) The activity of purified SHRC from WASH knockout MEFs reconstituted with the indicated HA-GFP-WASH variants was examined by pyrene-actin assembly assays.

(D) Cell lysates from reconstituted wild-type HA-GFP-WASH MEFs were treated with buffer or 3.5 μM AMSH deubiquitinating enzyme for 1 hr at 30 °C, subjected to anti-K63 ubiquitin chain IP, separated by SDS-PAGE, and immunoblotted for WASH (anti-HA).

(E) Cell lysates described in (D) were subjected to actin assembly assays on anti-HA beads as described in (A).
(F) Purified wild-type SHRC was treated with buffer or 3.5 μM AMSH for 1 hr at 30 °C and activity determined by pyrene-actin assembly assays.
(G) Model of MAGE-L2-TRIM27, Ube2O, and K63-ubiquitin regulation of SHRC activity and endosomal protein recycling. See also Figure S6.